BBA - Molecular Basis of Disease 1868 (2022) 166513

Contents lists available at ScienceDirect

BBA - Molecular Basis of Disease

journal homepage: www.elsevier.com/locate/bbadis

Substrate viscosity impairs temozolomide-mediated inhibition of glioblastoma cells' growth

Mateusz Cieśluk [a], Ewelina Piktel [b], Urszula Wnorowska [a], Karol Skłodowski [a], Jan Kochanowicz [c], Alina Kułakowska [c], Robert Bucki [a,*], Katarzyna Pogoda [d,**]

[a] Department of Medical Microbiology and Nanobiomedical Engineering, Medical University of Bialystok, PL-15222 Bialystok, Poland
[b] Independent Laboratory of Nanomedicine, Medical University of Bialystok, PL-15222 Bialystok, Poland
[c] Department of Neurology, Medical University of Bialystok, PL-15276 Bialystok, Poland
[d] Institute of Nuclear Physics Polish Academy of Sciences, PL-31342 Kraków, Poland

ARTICLE INFO

Keywords:
Rheology
Glioblastoma
Temozolomide
Polyacrylamide hydrogels
Viscoelasticity
Drug effectiveness

ABSTRACT

Background: The mechanical state of the extracellular environment of the brain cells considerably affects their phenotype during the development of central nervous system (CNS) pathologies, and when the cells respond to drugs. The reports on the evaluation of the viscoelastic properties of different brain tumors have shown that both tissue stiffness and viscosity can be altered during cancer development. Although a compelling number of reports established the role of substrate stiffness on the proliferation, motility, and drug sensitivity of brain cancer cells, there is a lack of parallel data in terms of alterations in substrate viscosity.

Methods: Based on viscoelasticity measurements of rat brain samples using strain rheometry, polyacrylamide (PAA) hydrogels mimicking elastic and viscous parameters of the tissues were prepared. Optical microscopy and flow cytometry were employed to assess the differences in glioblastoma cells morphology, proliferation, and cytotoxicity of anticancer drug temozolomide (TMZ) due to increased substrate viscosity.

Results: Our results indicate that changes in substrate viscosity affect the proliferation of untreated glioma cells to a lesser extent, but have a significant impact on the apoptosis-associated depolarization of mitochondria and level of DNA fragmentation. This suggests that viscosity sensing and stiffness sensing machinery can activate different signaling pathways in glioma cells.

Conclusion: Collected data indicate that viscosity should be considered an important parameter in *in vitro* polymer-based cell culture systems used for drug screening.

1. Introduction

An increasing number of reports focused on studying the mechanical properties of central nervous system (CNS) tissues have identified the viscoelastic behavior of the brain [1–11]. To date, it is known that the mechanical environment of brain tissue depends on age, gender, a specific region, or type of pathology developed within brain tissue, and was shown for instance to soften with age [5,12,13]. The stiffness of brain tissue is also affected by a variety of extracellular matrix changes, such as edema, angiogenesis, necrosis and matrix extracellular deposition [14–17]. Moreover, it has been found that in the early stages of the development of some diseases, changes in the stiffness of cells and brain tissue occur as a result of an increase in fibrosis and a decrease in cell necrosis, which are manifested at the molecular level as a diversified distribution of actin networks and changes in the cytoskeleton structure. Importantly, these alterations preceded any changes appearing during a histological assessment, which gives them highly-sensitive diagnostic potential [18,19]. It should be recognized that data reported in the

* Correspondence to: R. Bucki, Department of Medical Microbiology and Nanobiomedical Engineering, Medical University of Bialystok, Mickiewicza 2C, 15-222 Bialystok, Poland.
** Correspondence to: K. Pogoda, Department of Experimental Physics of Complex Systems (NZ52), Institute of Nuclear Physics Polish Academy of Sciences, Radzikowskiego 152, 31-342 Kraków, Poland.
E-mail addresses: mateusz.ciesluk@umb.edu.pl (M. Cieśluk), ewelina.piktel@umb.edu.pl (E. Piktel), urszula.wnorowska@umb.edu.pl (U. Wnorowska), karol.sklodowski@umb.edu.pl (K. Skłodowski), jan.kochanowicz@uskwb.pl (J. Kochanowicz), alakul@umb.edu.pl (A. Kułakowska), buckirobert@gmail.com (R. Bucki), katarzyna.pogoda@ifj.edu.pl (K. Pogoda).

https://doi.org/10.1016/j.bbadis.2022.166513
Received 7 March 2022; Received in revised form 16 July 2022; Accepted 29 July 2022
Available online 3 August 2022

literature show significant differences in the viscoelastic properties of the brain not only due to the heterogeneous nature of brain tissue but also as a result of testing conditions and methods that apply forces at different scales and frequencies [20]. Therefore, there are no generally accepted trends in mechanopathological changes of the brain tissue, like the ones established *e.g.*, in breast cancer, where it is believed that tumor mass is always stiffer than normal breast tissue [3,7–10,21–23]. Nevertheless, the sum of these reports highlights the unique softness of the brain tissue with the shear modulus (G′) on the order of hundreds of pascals accompanied by high viscosity, described by loss modulus (G″) that can be up to 10–20 % of G′ [24,25]. This highly fragile structure needs to be particularly protected, therefore it floats in jelly-like fluid inside the skull. The existence of the rigid and uncompressible boundaries around the brain implicates a significant increase in interstitial pressure and solid tissue stress whenever abnormal cells form and tumor mass starts to grow [26]. Deformed brain tissue responds differently when compressive or tensile forces appear, with the effect of tissue compression mostly studied and recognized to cause tissue stiffening up to three orders of magnitude within the range of compressive stresses reported *in vivo* [8]. Such mechanical response of the brain tissue implicates that *in vivo* single brain cells must adopt viscoelastic properties unlike the ones delivered from *ex vivo* low strain measurements of the brain tissue. The main driving force in the development of bioinspired compliant cell culture platforms is the observation that tissue cells can sense and respond to mechanical stimuli generated in their microenvironment. The typically used tissue culture plastic or glass are rigid materials with both mechanical and biochemical properties far from physiological relevance. Therefore, studies of brain-originated cells on soft, viscoelastic substrates that consist of naturally occurring extracellular matrix (ECM) proteins are especially emerging. Up till now, stiffness of the cellular microenvironment was recognized as the main factor that controls brain-derived cells phenotype, proliferation, migration, and response to treatment [27–30]. For this reason, many protocols describing the synthesis of polymer- and biopolymer-based hydrogels with precisely controlled elasticity were developed with water-swollen, crosslinked polyacrylamide hydrogels being the most common [31]. Recent studies on biological tissue rheology suggest that not only elasticity but also viscosity is a significant contributor to multiscale tissue biomechanics, with viscous properties responsible mostly for dissipating mechanical strain energy and their time- or strain-rate dependence [32]. As a consequence, materials with a linear elastic mechanical response, like crosslinked polyacrylamide hydrogels, are not optimal substrates to evaluate cell-ECM mechanical interactions, mechanopathology development, and effectiveness of drug treatment. To fill this gap, the synthesis of viscoelastic polyacrylamide hydrogels with independently tunable elasticity and viscous dissipation were recently proposed [33–35]. Controlled manipulation of polyacrylamide viscosity was possible due to partial exchange of water in pre-polymerized hydrogel mix with linear polyacrylamide chains that are confined in polyacrylamide elastic network during polymerization. Such a procedure allows synthetizing polyacrylamide hydrogels with similar elastic properties and various viscous contributions, giving rise to studies on the role of substrate viscosity in cell life and fate [34].

Glioblastoma (GB) is a malignant high-grade astrocytoma with a median survival of 7–18 months and the highest occurrence in 45–70 years old [36–38]. The standard treatment for glioblastoma is surgery [39], nevertheless, due to the poor prognosis of GB, the treatment and determination of the extent of resection to increase the general survival of patients remains to be a widely researched topic. With newly diagnosed glioblastoma there is an option of surgical resection of a tumor with additional radiation therapy and chemotherapy, which prolong the survival up to 12–18 months [40]. Currently, there are only three chemotherapeutics used to treat GB – temozolomide (TMZ), bevacizumab (BVC), and lomustine [41,42]. BVC is only used as a last-line treatment for GB following the failure of radiotherapy, temozolomide, and lomustine [43]. Lomustine is also used in recurrent GB and is currently being tested for primary GB along with TMZ with promising results for improved overall survival [44]. TMZ is a monofunctional DNA alkylating agent of the imidazotetrazine class characterized by lipophilic properties and oral bioavailability. Due to the more alkaline pH of brain tumors when compared to healthy tissue, TMZ is more actively accumulated within tumor tissue making it a favorable option for GB treatment [45,46]. Apart from this, multiple numbers of other chemotherapeutic agents have been suggested as a possible treatment of glioblastomas [47–49], including procarbazine, cisplatin, carboplatin, cediranib, vatalanib, sunitinib, nevertheless, satisfactory *in vitro* results have not been translated into clinical trials, preventing their introduction into clinical use [47–54]. The sum of the reports from brain biomechanics studies strongly suggests that this may have been due to a failure to account for changes in the viscoelastic characteristics of the extracellular environment and how stiffness and viscosity parameters affect cell behavior and its response to chemotherapeutic intervention. In this study, we attempted to understand this phenomenon using TMZ as a model anticancer agent. By matching up viscoelastic properties of the hydrogel substrates to freshly isolated brain tissues, we evaluated the role of substrate viscosity on the therapeutic effect of TMZ. We indicated that viscoelasticity has a significant impact on glioblastoma cells treatment efficacy and should be considered when drug-screening platforms are designed and new substances to cause therapeutic effects are tested.

2. Materials and methods

2.1. Rat tissue samples

Three samples of whole brains were collected from 6–week old female Wistar (Cmdb:Wi) rats, housed under standard conditions of temperature, nutrition, and light in the animal facility of the Experimental Medicine Center, Medical University of Bialystok. Acquired tissues were immediately placed into tubes filled with MACS tissue storage solution (Miltenyi Biotec, Germany) and transported on ice (~4 °C) for an average of 30 min before rheological measurements were carried out.

2.2. Tissue sample preparation

From each material, thick (~2–3 mm) slices around Ø8 mm were cut with a punch-out under liquid conditions. The prepared samples were placed onto the sandpaper glued with tape to the rheometer plate and rheological measurements were carried out at room temperature (20 °C).

2.3. Hydrogel preparation

The preparation of the PAA hydrogels consists of several preparatory steps before the actual synthesis of the gel [34]: (i) adhesive coverslips preparation, (ii) non-adhesive coverslips preparation, (iii) polymerization of linear PAA (viscous part of the final gel), (iv) polyacrylamide elastic network polymerization and (v) protein attachment to the gel surface. In detail, the preparation of viscoelastic polyacrylamide hydrogels was firstly described in the early work of Charrier E. et al. [34]. Briefly, adhesive coverslips are immersed in 5 % (3-Aminopropyl) triethoxysilane (APTES) (Merck, Germany) in distilled water (dH_2O) for 30 min, washed 3–5 times in dH_2O, and then immersed in 0.5 % glutaraldehyde (Merck, Germany) in dH_2O for 1 h. After that, coverslips are air-dried and stored preferably under a vacuum. Then, non-adhesive coverslips are immersed in 5 % Surfasil Siliconizing Fluid (Thermofisher Scientific, USA) in acetone for 10 s, rinsed with clean acetone, and subsequently methanol. The final step is to air-dry and store coverslips at room temperature. Linear PAA chains are polymerized in a 50 ml glass bottle by mixing 40 % acrylamide solution (Bio-Rad), dH_2O, TEMED (Bio-Rad), and 10 % ammonium persulfate (APS) (Bio-Rad) according to the recipe in Table 1 for 1 h at 37 °C. The final solution of linear PAA

Table 1
Composition of linear polyacrylamide solution in [ml] for the final volume of 10 ml.

40 % acrylamide solution	H_2O	TEMED	10 % APS
1.25 ml	8.72 ml	5 μl	25 μl

should be homogenous and highly viscous. For long time storage, it should be protected from light and stored at 4 °C.

Polyacrylamide hydrogels are prepared by mixing acrylamide and bis-acrylamide solution (Bio-Rad) according to the recipe in Table 2. Identical concentrations of acrylamide and bis-acrylamide in both elastic and viscoelastic hydrogels guarantee the formation of a similar crosslinked PAA network, while the addition of linear PAA chains allows for an increase in hydrogels viscosity. For final hydrogel formation, 200 μl of the gel mix must be deposited on a glutaraldehyde-treated coverslip and covered with a siliconized coverslip. After a minimum of 15 min, dH_2O can be added to the sides of the hydrogels to prevent drying and further damage. After another 15 min, the top coverslip can be removed and hydrogel substrates immersed in dH_2O.

Both elastic and viscoelastic hydrogels need to be coupled with extracellular matrix protein to allow for cell adhesion. Firstly, the gels are rinsed with 50 mM HEPES at pH = 8.2 and covered with 5 mM sulfosuccinimidyl 6–(40-azido-20-nitrophenyla-mino)hexanoate (sulfo-SANPAH) solution in 75 % H_2O and 25 % DMSO. Subsequent sulfo-SANPAH activation requires UV irradiation under aseptic conditions for 15 min. The activated gel surface needs to be rinsed several times in HEPES and finally coated with 0.1 % collagen I solution for 2 h to obtain a homogenous protein monolayer [35].

2.4. Rheological measurements

Rheological properties of tissues were investigated using an MCR302 rheometer (Anton Paar, Austria) in a plate-plate geometry, wherein the diameter of the upper plate was 8 mm. All tests were performed at 20 °C. To avoid sample slippage during the experiments, tissue pieces were placed on sandpaper (P800), which was glued to the rheometer bottom plate. During the test, a sample humidity hood was used to prevent temperature changes and sample drying.

Two kinds of tests were performed for the brain tissues. The first one included oscillating shear deformation of the tissue with 2 % constant shear amplitude (and constant frequency of 2 Hz) and simultaneous uniaxial compression, which was applied by decreasing the distance between the parallel plates (gap height) in the range of 0–20 % of the sample initial height with a 10 % increment. This allowed us to obtain G′ and G″ values in compressed and uncompressed states. The second was a stress relaxation test performed by application of a 50 % shear strain at a constant rate to achieve the desired elongation. Then the strain was held constant for 240 s and relaxation modulus G(t) was registered as a function of time [55].

For the rheological characterization of elastic and viscoelastic hydrogels, the upper plate diameter was changed to 20 mm, and the gap height was set to 1 mm, which requires 325 μl volume of the gel mix to be placed between the rheometer plates. Since polymerizing gel mix adheres to rheometer plates, the usage of sandpaper was unnecessary. Rheological testing of the hydrogels allowed to follow storage (G′) and loss (G″) moduli evolution during polymerization of elastic and viscoelastic hydrogels as well as to determine relaxation modulus G(t) over time.

2.5. Cell culture

Human brain glioblastoma cells LN-18 (ATCC® CRL-2610™) and LN-229 (ATCC® CRL-2611™) were cultured in DMEM complemented with 10 % fetal bovine serum (FBS), 4 mM/L glutamine, and 1 % of antibiotics (penicillin, streptomycin, amphotericin B) at 37 °C (5 % CO_2). For experiments, cells were seeded at a density of 50 000 cells per hydrogel and incubated for 2 days to ensure attachment and appropriate cell spreading. After 48 h cells were treated with TMZ at doses varying from 50 to 2000 μM for 72 h. Doses of 50, 200, 500, 1000, and 2000 μM were used to test proliferation capabilities and cell morphology after TMZ treatment while 1000, 1500, and 2000 μM doses were used to evaluate TMZ cytotoxicity.

2.6. Proliferation of cells

The total number of LN-18 and LN-229 glioblastoma cells capable of proliferation after TMZ-treatment (50–2000 μM) when grown on tissue plastic surface, as well as on elastic and viscoelastic hydrogels, was explored by flow cytometry using Muse® Count & Viability Kit according to manufacturer's guide, as demonstrated previously [56]. Moreover, the expression of Ki-67 protein, recognized as a marker of cellular proliferation, was analyzed in TMZ-treated cells using Muse® Ki67 Proliferation Kit.

2.7. Cell morphology assessment

Bright-field images of LN-229 cells after 72 h post-TMZ treatment that grow onto elastic and viscoelastic hydrogels were acquired using Zeiss Axio Vert.A1 inverted microscope with Axiocam 208 colour camera (Zeiss, Germany). The ImageJ software was employed to calculate cell shape descriptors (area, perimeter, aspect ratio, roundness) with a manual calculation of the cell blebs. Images of treated and untreated cells were taken using 40× objective from 3 different sample preparations. 100 cells per condition were randomly selected and analyzed. The ImageJ analysis was calibrated using a scale bar within the microscope software. The default unit was set as 1 μm, thus the area was measured in μm^2, perimeter in μm, and aspect ratio as:

$$\frac{[Major\ axis]}{[Minor\ axis]} \tag{1}$$

where the major and minor axis is the primary and secondary axis of the best fitting ellipse in the measured area. Cell roundness was calculated as follows:

$$4 \times \frac{[Area]}{\pi \times [Major\ axis]^2} \tag{2}$$

where the area is the area of selection and the major axis is the primary axis of the best fitting ellipse in the measured area.

Table 2
Composition of elastic and viscoelastic polyacrylamide gels in [μl] for a total of 500 μl volume.

	G′ [kPa] G″ [Pa]	40 % acrylamide solution [μl]	2 % bis-acrylamide solution [μl]	H_2O [μl]	TEMED [μl]	10 % APS [μl]	Linear polyacrylamide [μl]
Elastic hydrogel	1.57 5	69	25	401	1.25	3.75	–
Viscoelastic hydrogel	1.69 333	69	25	80	1.25	3.75	321

2.8. Cell apoptosis analysis

The induction of apoptosis in TMZ-treated cells was estimated using Muse® Caspase-3/7 Kit according to the manufacturer's guidelines. Briefly, collected cell populations were exposed to DEVD peptide substrate-based Caspase 3/7 reagent for 30 min at 37 °C, co-stained with 7-aminoactinomycin D (7-AAD) to detect caspase-positive, non-viable cells and analyzed by Muse Cell Analyzer (Luminex Corporation, USA).

2.9. Mitochondrial transmembrane potential analysis

The TMZ-induced alterations in the mitochondrial potential of glioblastoma cells were measured using the NucleoCounter® NC-3000™ (Luminex Corporation, USA) fluorescence image cytometer, according to the previously published protocol [57]. For this purpose, LN-229 cells treated with TMZ were incubated with Solution 7 (at a final JC-1 concentration of 2.5 μg/ml) for 10 min at 37 °C, washed thoroughly with PBS, resuspended in Solution 8 (1 μg/ml DAPI in PBS), and analyzed immediately by NucleoCounter® NC-3000™ software [58,59].

2.10. Evaluation of DNA fragmentation

Detection of alterations in DNA content in treated brain cancer LN-229 cells was performed using a DNA Fragmentation Assay Kit prepared for NucleoCounter® NC-3000™ system (ChemoMetec, Denmark), following the manufacturer's instructions. LN-229 cells were treated with tested agents at the doses of 1000, 1500, and 2000 μM for 72 h, harvested, washed, and fixed in 70 % ethanol for 12 h. Ethanol-suspended cells were centrifuged for 5 min at 500*g*, resuspended in Solution 3 containing 1 μg/ml DAPI and 0.1 % Triton X-100 in PBS, loaded onto an NC-Slide and DNA content histograms were collected [57].

2.11. PI3K activation

Measurement of PI3K activation in glioblastoma cells treated with TMZ was carried out using Muse™ PI3K/MAPK Dual Pathway Activation Kit as guided by the manufacturer. Briefly, TMZ-treated cells after 72 h incubation were washed with PBS, harvested, and fixed for 10 min on ice. After rinsing with PBS, cells were permeabilized with Permeabilization Buffer for 5 min on ice followed by washing and incubation of cells with antibody cocktail for 30 min at room temperature in the dark. Samples were analyzed using a Muse™ Cell Analyzer.

2.12. Statistical analysis

Statistical significance was determined using a two-tailed Student's *t*-test. Statistical analyses were performed using OriginPro 9.9 (OriginLab Corporation, USA). P-values < 0.05 were considered to be statistically significant. Average values were presented as mean ± SD, where mean is the average value for the group and SD is the standard deviation. Each of the tested conditions was performed in triplicate.

3. Results

3.1. Rheological measurement of brain tissues and synthesized PAA gels

The schematic representation of the experimental setup is presented

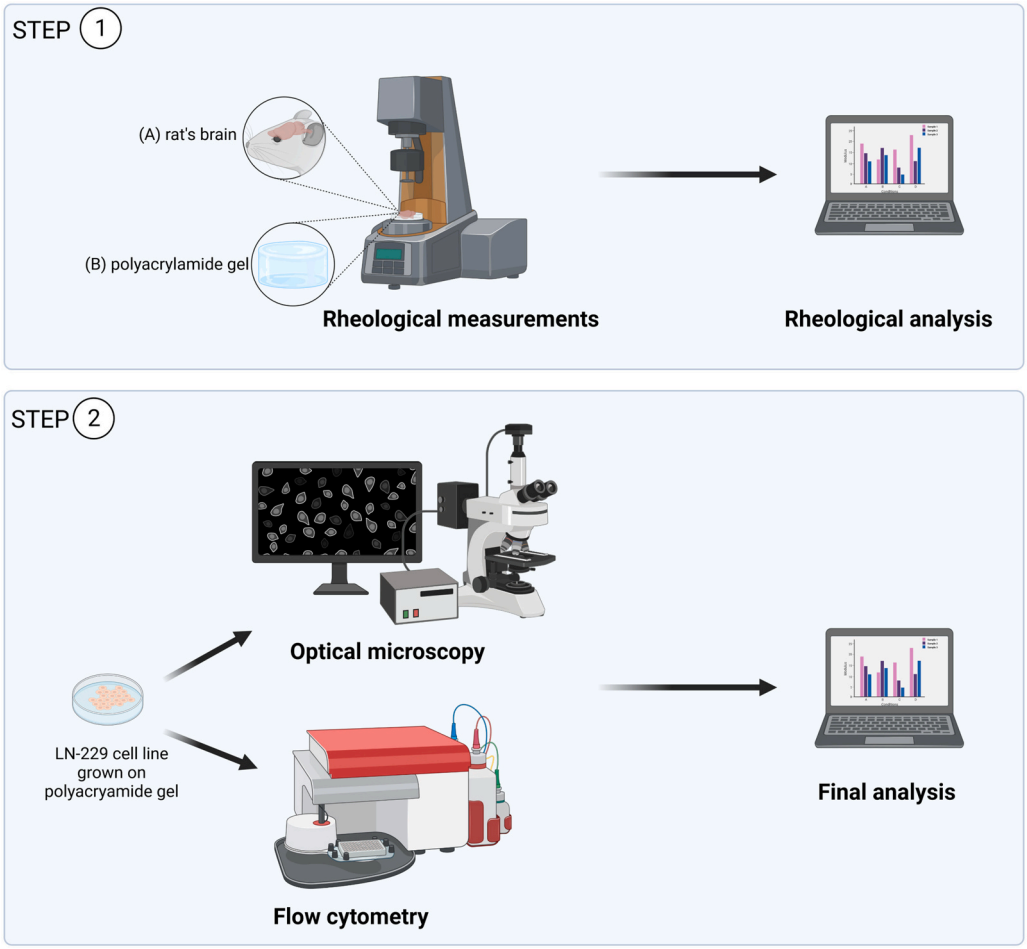

Fig. 1. Schematic representation of the experimental design.

in Fig. 1. First, rheological measurements of the freshly isolated rat brain tissue were performed to optimize polyacrylamide hydrogels synthesis. Storage G′ and loss G″ moduli of the tissues were characterized at low strain measurements without uniaxial compression as well as at 10 % and 20 % compressive stress (Fig. 2A). Storage modulus (G′) without compression was determined to be equal to 642 ± 84 Pa and loss modulus (G″) 280 ± 38 Pa (3 subjects measured). The G′ value upon application of 10 % compression increased to 1175 ± 45 Pa and G″ 449 ± 37 Pa, while at 20 % compression it reached 1742 ± 47 Pa for G′ and 575 ± 77 Pa for G″. The ratio of G″/G′ was equal to 44 ± 2 %, 38 ± 3 %, and 34 ± 3 % for non-compressed, 10 %, and 20 % compression, respectively. The obtained G′ and G″ values served for optimization of elastic and viscoelastic polyacrylamide hydrogels synthesis. We aimed to prepare hydrogels that can mimic the mechanical properties of the

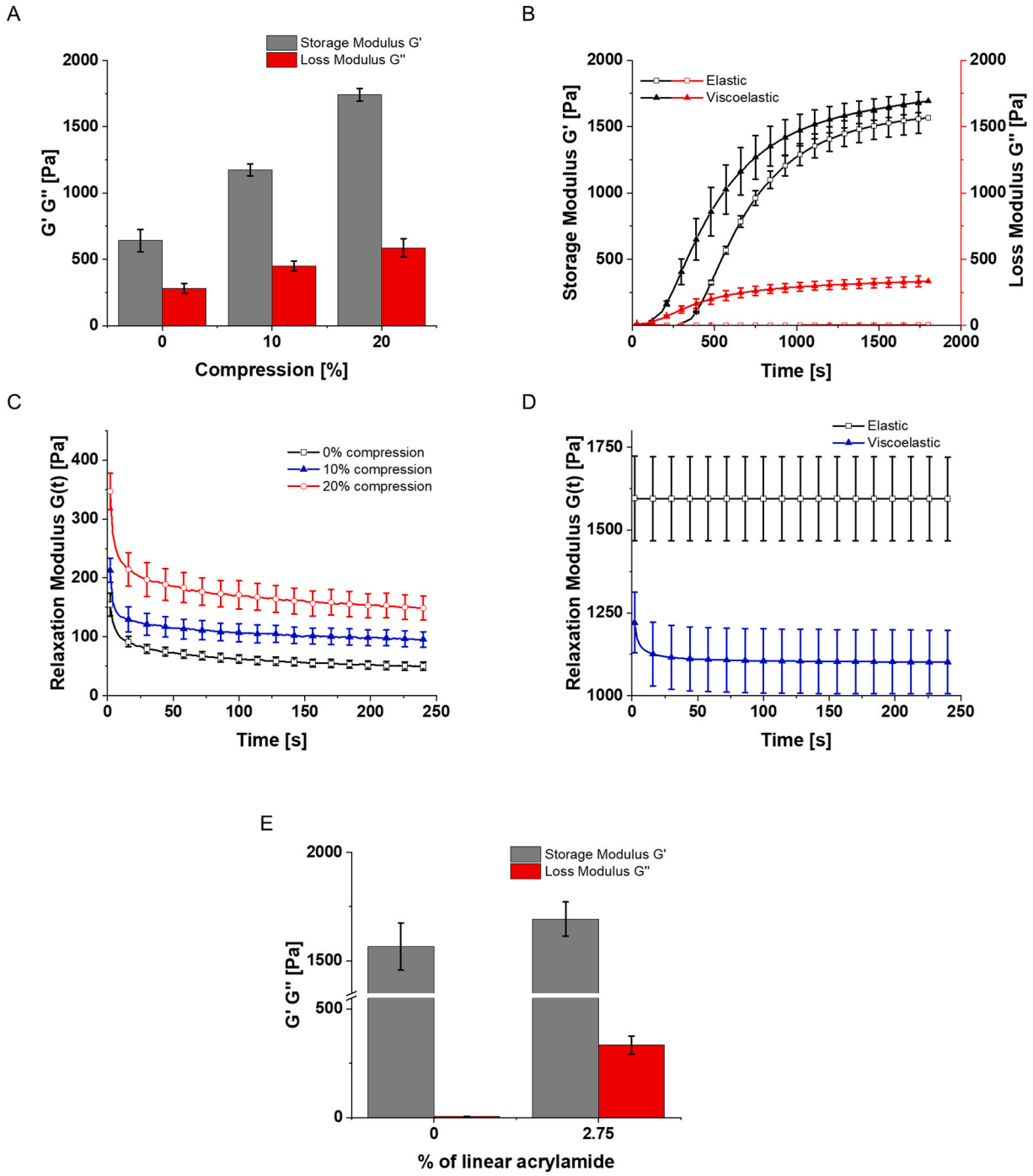

Fig. 2. Rheological properties of the healthy rat brain and polyacrylamide gels. A – Values of G′ and G″ as characterized by a 2 % oscillating shear stress at a frequency of 2 Hz and 2 % strain for different compressions B – Evolution of G′ and G″ during the polymerization of elastic and viscoelastic gels: G′ and G″ both increase during the Formation of the branched PAA network. G′, black (left axis); G″, red (right axis). C – Stress relaxation of healthy rat brain under compression: evolution of the shear modulus over time under a 50 % strain. D – Average plots of the stress relaxation of elastic and viscoelastic gels containing 0 and 2.75 % linear polyacrylamide: evolution of the shear modulus over time under a 50 % strain. Error bars represent the standard deviation. E – Average values of G′ and G″ as characterized by a 2 % oscillating shear stress at a frequency of 2 Hz and 2 % strain; $n = 4$ for elastic and 3 for viscoelastic gel. Error bars represent the standard deviation. (For interpretation of the references to colour in this figure legend, the reader is referred to the web version of this article.)

brain tissue with the possibility of precisely controlling their elastic and viscous properties. To study the role of substrate viscosity in cellular drug response we have polymerized purely elastic and viscoelastic polyacrylamide hydrogels with similar stiffnesses. Fig. 2B shows the evolution of G′ and G″ during the process of gel polymerization between the rheometer plates. Our elastic hydrogel has G′ equal 1567 ± 109 Pa and G″ as low as 4.7 ± 0.4 Pa while viscoelastic hydrogel has similar elastic properties with G′ equal 1693 ± 79 Pa and much greater viscosity G″ equal to 334 ± 42 Pa. Such preparation allowed us to reach G″/G′ ratio of 19 % for the viscoelastic hydrogel, which is the highest we can achieve using this protocol [35]. Obtained mechanical properties of the hydrogels are within the range of G′ and G″ values of the soft tissues, especially the brain under moderate compression. Fig. 2C depicts stress relaxation of the brain tissues after application of the constant strain. Such behavior is typical for viscoelastic materials that behave in a nonlinear fashion. Therefore, purely elastic polyacrylamide hydrogels do not exhibit such behavior, but the incorporation of the long polyacrylamide chains into the elastic hydrogel network allows to create viscoelastic polyacrylamide that relax stresses similarly to biological tissues (Fig. 2D).

3.2. TMZ-treated glioblastoma cells exhibit greater proliferatin when cultured on viscoelastic than elastic matrices

To compare the changes in the proliferation of glioblastoma cells grown on plastic surfaces and elastic or viscoelastic gels, flow cytometry was engaged. As demonstrated in Fig. 3A, despite the seeding of cells at the same density, the total number of grown cells differed significantly between experimental settings and was counted as 18.7×10^4, 8.09×10^4 and 6.45×10^4 for LN-18 and 34.9×10^4, 5.8×10^4 and 5.5×10^4 for LN-229 when grown on tissue culture (TC) plastic, elastic and viscoelastic hydrogels, respectively. Accordingly, a statistically significant decrease in cell proliferation on the TC plastic *versus* both hydrogel types was observed, while significant difference between elastic and viscoelastic hydrogels was shown only for LN-18 cell line. In another experimental set, TMZ-induced inhibition of cellular proliferation was estimated when cells were maintained on elastic and viscoelastic substrates. As demonstrated in Fig. 3B, the effect of temozolomide

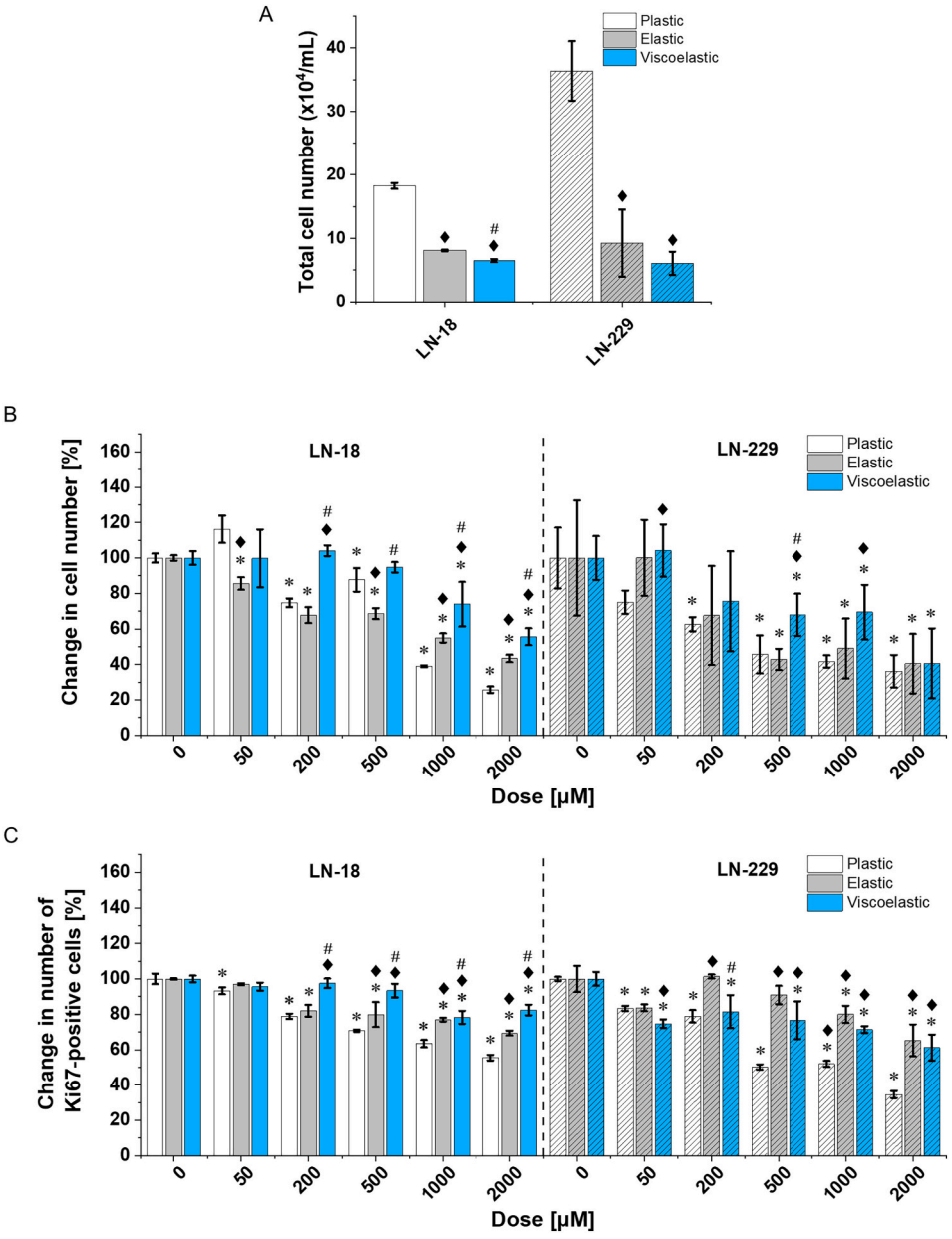

Fig. 3. Proliferation capabilities of LN-18 and LN299 cells treated on plastic (white), elastic (grey) and viscoelastic gels (blue). A – Proliferation capability of LN-18 and LN229 cells on the surface of cell culture-treated plates, elastic and viscoelastic gels B – Percentage changes in proliferation of cells on the surface of plastic, elastic and viscoelastic gels. C – Percentage changes in number of Ki67-positive cells on the surface of plastic, elastic and viscoelastic gels. Error bars represent the standard deviation. The unpaired Student's *t*-test was used to confirm statistical differences (denotations: * - $p \leq 0.05$; * - in comparison to control; ◆ - in comparison to plastic; # - in comparison to the respective dose on gels). (For interpretation of the references to colour in this figure legend, the reader is referred to the web version of this article.)

treatment on LN-18 is more prominent in cells grown on TC plastic and significantly lower when cells were cultured on hydrogels, particularly for higher doses (1000–2000 μM) of TMZ. Importantly, at TMZ concentration range of 200–2000 μM TMZ, cells were significantly less affected by anti-cancer treatment when maintained in the environment of higher viscosity. Similar observations were noted when investigating LN-229 cells. The considerable effect of TMZ was noted at the lowest dose of 50 μM TMZ, when cells were grown on TC plastic, while the same dose did not affect cells grown on elastic and viscoelastic substrates. TMZ was less effective against glioblastoma cells grown on viscoelastic

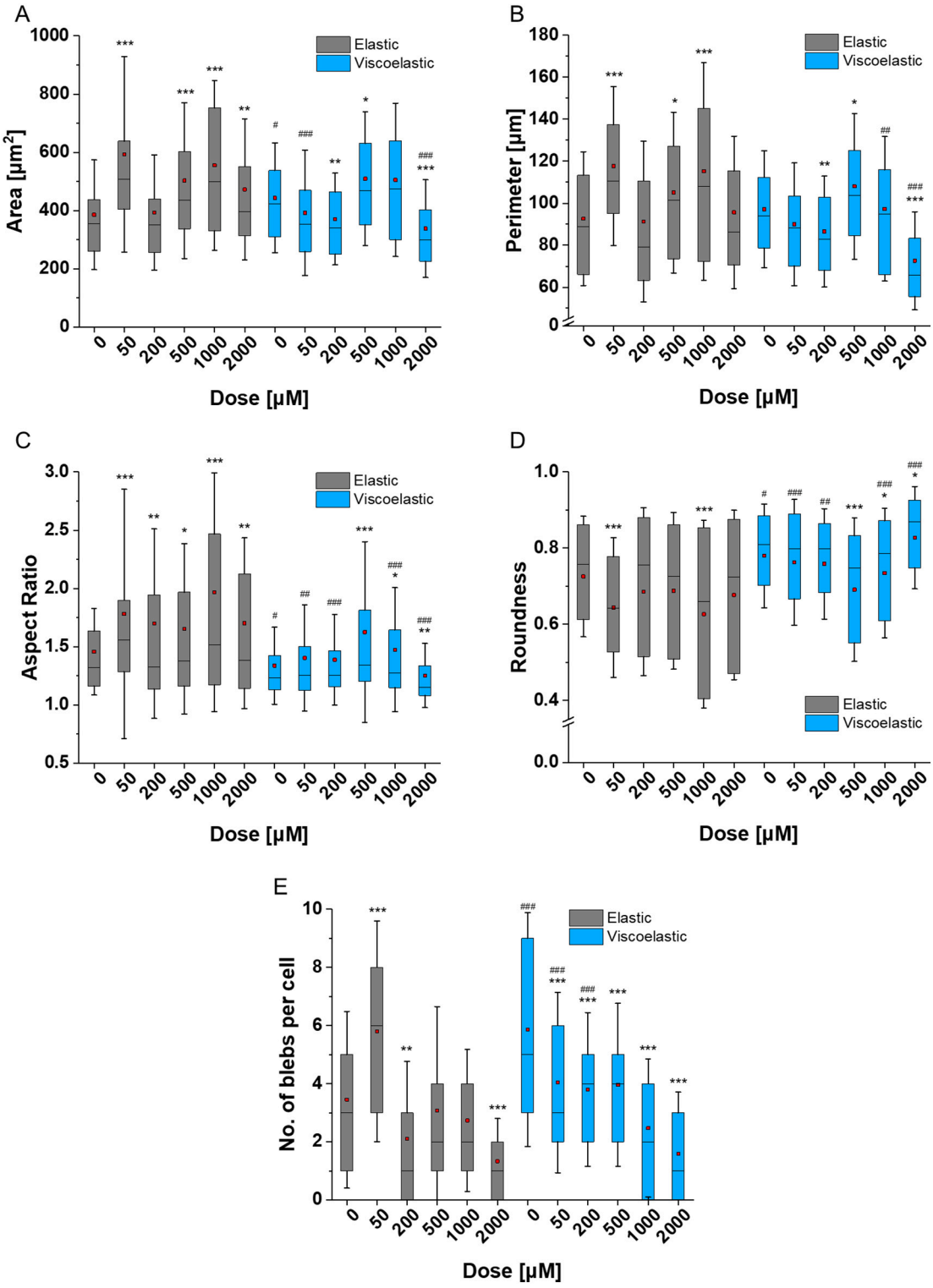

Fig. 4. Cell characteristics after 72 h temozolomide treatment grown on elastic (grey) and viscoelastic (blue) polyacrylamide hydrogels. A – Cell spread area. B – Cells' perimeter. C – The aspect ratio of the fitted ellipse (*i.e.* [Major axis]/[Minor axis]). D – Roundness of the cells (4 × [Area]/(π × [Major axis]2)). E – Number of blebs per cell. $n = 100$ cells per condition; red square – average value; whisker – standard deviation. The unpaired Student's *t*-test was used to confirm statistical differences (denotations: * #,$p \leq 0.05$; ** ##,$p \leq 0.01$; *** ###,$p \leq 0.001$; * - in comparison to control; # - in comparison to the respective dose). (For interpretation of the references to colour in this figure legend, the reader is referred to the web version of this article.)

than elastic substrates, which can be seen at the 500 μM TMZ dose used. At the highest TMZ concentrations (2000 μM) treatment was equally effective for cells grown on all substrate types.

The impact of viscosity on proliferation capability of cells was also confirmed when measuring the number of cells with the positive expression of Ki-67 protein, widely recognized as a marker of cellular proliferation [60,61]. As shown in Fig. 3C the highest number of Ki-67 positive cells was noted when TMZ was administrated to the cells grown on viscoelastic hydrogels. This tendency was noted particularly for LN-18 and at lesser extent for LN-229 cells.

3.3. Glioma cells grown on viscoelastic substrates display different morphological characteristics than those on elastic substrates

The differences in morphology of cells grown on elastic and viscoelastic hydrogels were explored by the calculations of such parameters as cell area (Fig. 4A), cell perimeter (Fig. 4B), an aspect ratio of the cell's fitted ellipse (Fig. 4C), as well as cellular roundness (Fig. 4D) and manual counting of the number of blebs per cell (Fig. 4C). Collected data indicate that cells grown on viscoelastic substrates and treated with TMZ display a smaller cell spread area in comparison to cells maintained on the elastic matrices – for instance, cells treated with 1000 μM TMZ have an average spread area of 505 ± 263 μm^2 and 555 ± 291 μm^2 for cells grown on viscoelastic and elastic hydrogels, respectively (Fig. 4A). Accordingly, TZM-treated cells were smaller in perimeter and this difference was considered statistically significant (Fig. 4B). Fig. 4C presents the aspect ratio of the cell's fitted ellipse. As shown, cells on elastic hydrogel with TMZ treatment are significantly different from the control samples, and in all cases, except the control sample, the ratio is above 1.5, whereas, cells on viscoelastic hydrogel were more round with a ratio below 1.5 and closer to 1.25. This observation was confirmed by the calculation of cellular roundness with cells grown on viscoelastic hydrogels being overall more round than grown on elastic ones (Fig. 4D). Fig. 4E presents the average number of blebs per cell with 3.5 ± 3.0 and 5.9 ± 4.0 untreated cells grown on elastic and viscoelastic substrates, respectively. At high TMZ doses, a number of blebs per cell is comparable and drops to 1.3 ± 1.5 for elastic and 1.6 ± 2.1 for viscoelastic hydrogel.

3.4. Cells grown on viscoelastic hydrogels are less affected by TMZ treatment

To explore the ability of TMZ to induce cytotoxic effects in glioblastoma cells maintained on plastic or hydrogels, the following

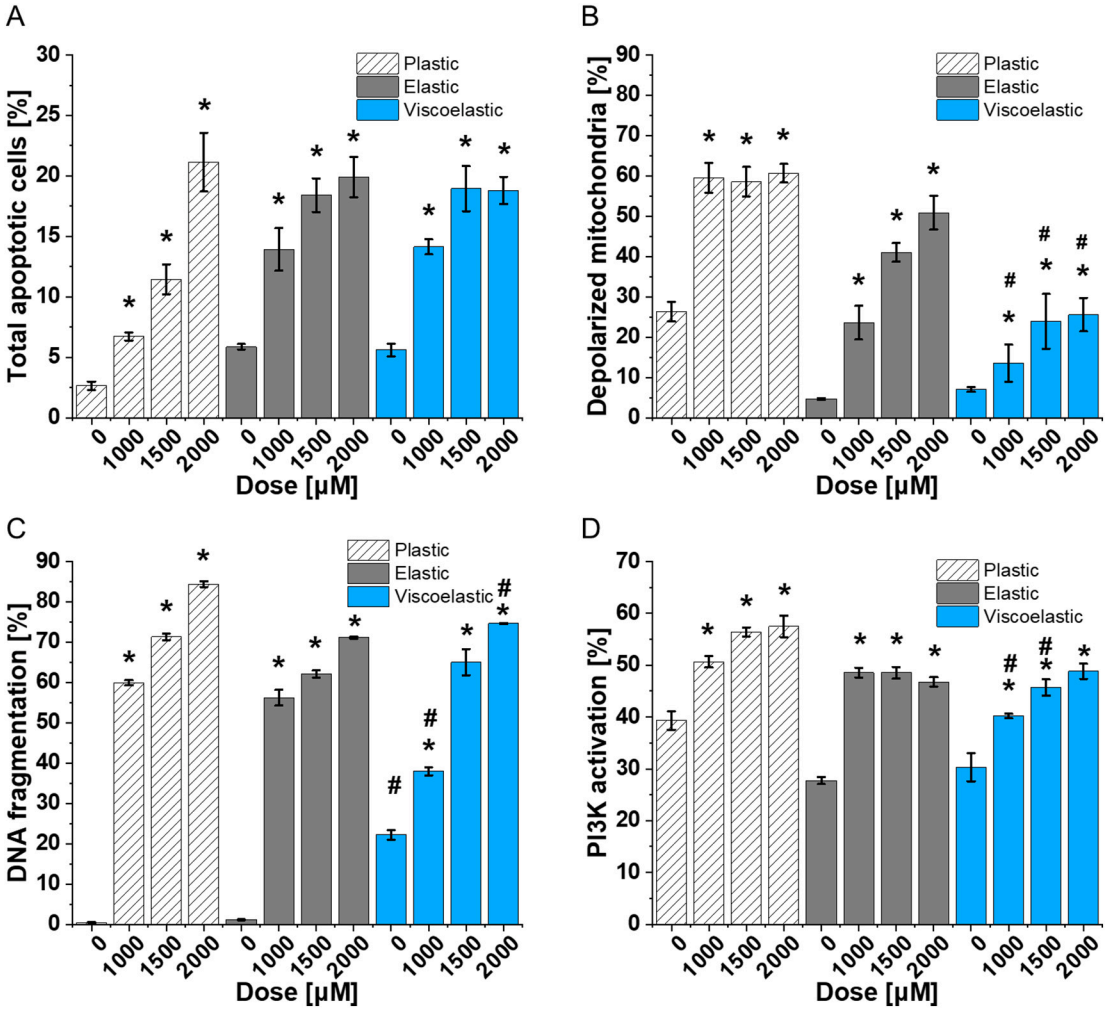

Fig. 5. Cytotoxic effect of temozolomide against LN299 cells treated on plastic (white), elastic (grey), and viscoelastic gels (blue). A – Total apoptotic LN299 cells treated on the surface of cell culture-treated plates, elastic and viscoelastic gels B – Depolarized mitochondria of LN229 cells on the surface of plastic, elastic and viscoelastic gels. C – DNA fragmentation of LN229 cells on the surface of plastic, elastic and viscoelastic gels D – PI3K pathway activation of LN229 cells on the surface of plastic, elastic and viscoelastic gels. Error bars represent the standard deviation. The unpaired Student's *t*-test was used to confirm statistical differences (denotations: *,$p \leq 0.05$; * - in comparison to control; # - in comparison to the respective dose on elastic gel). (For interpretation of the references to colour in this figure legend, the reader is referred to the web version of this article.)

parameters were quantified: (i) number of apoptotic cells, (ii) level of mitochondria depolarization, (iii) intensity of DNA fragmentation, and (iv) activation of PI3K signaling. The results of these analyses are presented in Fig. 5. As demonstrated, despite the lack of differences in the number of apoptotic cells detected on plastic and hydrogels (Fig. 5A), we have recorded a significant decrease in mitochondrial depolarization and DNA fragmentation, when TMZ was subjected to the cells grown on viscoelastic substrates. More quantitively, the percentage of cells with impaired mitochondrial function was two-fold lower for cells grown on viscoelastic substrates in comparison to both control and respective dose on the purely elastic ones (Fig. 5B). DNA fragmentation was also lower for cells in a viscoelastic environment and this effect was particularly prominent for 1000 μM dose of TMZ (Fig. 5C). Statistically significant differences were also noted when PI3K pathway activation was explored. As shown in Fig. 5D, the highest PI3K activation was achieved on a TC plastic substrate and it was quantified as 58 ± 2 % for 2000 μM TMZ treatment. In comparison, for cells cultured on hydrogel matrices, the level of PI3K activation was not higher than 49 ± 1 %. This signaling point was also less activated in cells collected from viscoelastic hydrogels, than in those collected from the elastic ones.

4. Discussion

Research on malignant brain tumors, such as glioblastomas with altered microenvironmental structure and biomechanics, allow us to constantly broaden our knowledge of their invasiveness and motility [27,62] leading to a better understanding of these aggressive and rapidly lethal cancers. Interest in the mechanics of brain tissue has recently revived, and although a convincing amount of data has been collected to describe the response of brain tissue to mechanical stresses and characterize their viscoelastic nature, there is still much work to be done to accurately understand this intricate structure due to *e.g.* difficulties with human sample acquisition and limitations of *ex vivo* studies [3,6,8,12,22,23,63,64]. New developments in measurement techniques, including magnetic resonance elastography (MRE), have great potential to non-invasively measure tissue properties *in vivo*, which may be used in the future for diagnostic purposes and give extra insight into traumatic brain injuries and neurological diseases like tumors (*i.e.*, glioblastoma) [4,5,7,15,64–70]. However, *ex vivo* measurements of the brain tissue using, for example, a rheometer may still help us to understand tissue biomechanics that could be transposed to 2D and 3D cell cultures to mimic more physiological conditions [8,27,62,71].

In this study, we characterized rat brain tissues' rheological properties to better understand their viscoelastic nature and further optimize the preparation of polyacrylamide hydrogels to culture LN-18 and LN-229 glioblastoma cells and study the viscosity-dependent effects of TMZ treatment.

In previous research, various glioblastoma cell lines were grown on polymer-based gels with different stiffness and tested using atomic force microscopy to observe their local elastic properties [8,71]. Interestingly, it was reported that substrate stiffness and chemical signaling elicited the same cellular phenotype, which indicates that both mechanical and chemical aspects of the microenvironment can result in comparable cellular reactions [10,71]. It is established that cells respond to variations in substrate elasticity by modulating their stiffness and morphology alterations. Furthermore, migratory properties are stiffness-sensitive for some cancerous cell lines [28,62]. Moreover, an ever-growing number of reports indicate that apart from this, also other cellular effects are governed by substrate mechanical properties, such as cell cycle progression or proliferation capability. The first one was reported in mammary epithelial cells, smooth muscle cells, fibroblasts, and other non-neuroglial cells demonstrating that pathological ECM remodeling and stiffening of the microenvironment is a positive regulator of the cell cycle *via* integrin-dependent signaling to FAK, cyclin D1, and Rac [72]. Proliferation dependence on substrate changes was also recorded in the works of other authors [62,73,74]. One explanation is that the changes in cell cycle progression occur by alternations in mechanochemical response during mitosis. Secondly, extracellular matrix elasticity may regulate mitosis by synergistic activation of mechanotransductive and mitogenic signaling pathways [62]. Our results suggest that similar phenomenon might occur due to increased environmental viscosity. According to data presented in Fig. 3A, cells cultured on polyacrylamide hydrogels proliferate much slower than those growing on stiff TC plastic. Moreover, number of TMZ-treated cells expressing Ki-67 protein, which is a factor substantially expressed in cells that are cycling, but markedly suppressed in cells that are resting in the G0 phase [75], was found significantly varied between tested matrices (Fig. 3C). This finding might suggest substrate viscosity mitigates the cell cycle in drug-treated cells, however, we are fully aware, that such hypothesis needs to be tested in more detail with additional experimental settings.

Reports to date established that to properly conduct cell experiments, it is necessary to assure not only the optimal temperature conditions or the provision of adequate nutrients for growing cells, but also to consider the mechanical parameters of the extracellular environment that cells originate. The latter has become increasingly important in recent times considering that a variety of cytotoxic agents do not reach clinical effectiveness, despite the satisfactory results in *in vitro* settings, which could be determined by the inappropriate design of cell culture platforms [47–54]. Firstly, glioma or astrocyte cells are usually grown on stiff substrates such as glass or TC plastic that do not resemble the elastic properties of the soft tissues [8,71,76–78]. Secondly, even if microenvironmental elasticity is accounted the viscosity of ECM is often overlooked, and the amount of data indicating its importance for cell behavior is very limited. Another reason was that controlled incorporation of viscous properties to existing protocols of soft substrates formulation was difficult to achieve. Only recently, it was demonstrated that linear polyacrylamide chains entrapped inside the elastic polyacrylamide network can dissipate energy and thus become the viscous component that can be independently controlled [33]. Moreover, such modification did not affect the performance of adhesion proteins on the network of the viscoelastic gels but was reported to influence cell internal stiffness and differentiation. For this reason, it was suggested that viscous dissipation in biological tissues is a determinant of cell phenotype and tissue homeostasis [33]. A study by Charrier et al. authors demonstrated that 3 T3 fibroblasts grown on viscoelastic gels are characterized by increased cell motility when compared to those on elastic gels. At the same time, human airway smooth muscle (HASM) cells and cancerous 22Rv1 cells spread significantly less on viscoelastic gels than on elastic ones of similar storage modulus, which suggests that the storage and the loss moduli of the substrate are integrated through different signaling pathways within these cells [34]. Contrastingly, in a report by Cameron et al. mesenchymal stem cells grown on viscoelastic gels were noted to display increased proliferation and spread area in comparison to pure elastic ones [79]. In our study, we recorded an almost seven-fold change in proliferation between stiff TC plastic surfaces and elastic or viscoelastic polyacrylamide hydrogels. A similar effect was reported by other groups, *e.g.* primary adult dermal fibroblasts were shown to proliferate faster on stiff *versus* soft substrates [80]. The same phenomena were reported for primary myoblasts, mammary epithelial cells, vascular smooth muscle cells, and mouse embryonic fibroblasts [62,81,82]. At the same time, we detected no difference in proliferation capability of glioblastoma cells grown on elastic or viscoelastic gels (Fig. 3A) but a remarkable difference in cell morphology was observed and demonstrated in Figs. 4A-4E. Briefly, cells cultured on viscoelastic matrices displayed increased spread area and larger perimeter, decreased aspect ratio, increased roundness, as well as an enhanced number of blebs compared to cells grown on purely elastic substrates. This confirms that viscosity should be taken under the consideration in designing the 2D cell culture models.

Given that the microenvironmental viscoelasticity affects glioblastoma cells' properties, research focused on the influence of substrate

viscoelasticity along with drug treatment might help in understanding and future development of more efficient anti-glioma therapies. To date, only a few studies have shown the influence of the nanomechanical properties of the extracellular environment on the effectiveness of anticancer drugs. Between them, Feng J. et al. research group showed that breast cancer cells were more sensitive to antitumor drugs such as cisplatin and taxol on stiffer substrates and concluded that screening for antitumor drugs on plastic *in vitro* models might result in misleading information, which would also increase costs of research [83]. For the same reason, another group of researchers suggested 3D biomimetic models of selected tissue stiffness as an interface for drug testing [84]. Similar effects were recorded in colorectal cancer where reduction of liver metastasis stiffness improved the response to BVC [85]. In contrast to these reports, Lam et al. presented that metastatic breast tumor cells were undergoing paclitaxel-induced apoptosis earlier when an invasion was through soft collagen matrices, which suggested that stiffer matrices support cancer cells' dormancy for drug therapy, raising the probability of a future disease recurrence [84]. The stiffness-dependent response was also recorded for breast cancer cells and doxorubicin with increased resistance correlating with PDMS matrices stiffness increase [86]. Importantly, in one of the newer reports, Nicolas-Boluda et al. observed that the direct inhibition of factors affecting EMC stiffness and organization might be also translated into improved treatment response. In such aspect, inhibition of lysyl oxidase (LOS), *i.e.*, an ECM collagen fibers stabilizer, was reported to increase intratumoral T cell migration and infiltration and in further steps also improved response to anti-PD-1 treatment, particularly in early tumor stages [87,88]. Modulation of treatment outcome might be also influenced by altering collagen concentration within tumor tissue, which affect directly intracellular stiffness and motor activity [89]. Accordingly, changes in collagen concentration might impact paclitaxel, ROCK inhibitor, and MMP inhibitor effectiveness [89]. Thus, making a distinction in cell response to the drug in the varying environment could be essential for new treatment development that targets specific intracellular behavior associated with disease progression. However, the abovementioned research focused mostly on the role of elasticity, while exploration of both elastic and viscous properties of the ECM on drug efficiency is needed. According to our best knowledge, our study is the very first research focusing on this issue. As demonstrated, incorporation of the viscous elements to the hydrogel structure only slightly affects cell proliferation of untreated cells but displays a significant impact on TMZ cytotoxicity against LN-229 cells (Fig. 5). Interestingly, we have noted a comparable percentage of apoptotic cells in the TMZ-treated population (Fig. 5A), but at the same time, a level of depolarized mitochondria or fragmented DNA significantly differ (Fig. 5B and C), clearly indicating that ECM viscosity may limit the therapeutic effect of TMZ *via* these signaling pathways. It is established that temozolomide induces cell death effects in glioma cells by varied signaling routes, leading ultimately to apoptosis induction in TMZ-treated cells [90]. It is well-recognized that TMZ cytotoxicity is mediated by O6-guanine residues (O6-MeG), which is a mutagenic, carcinogenic and toxic lesion. Unrepaired O6-MeG during DNA replication mispairs with thymine, which activates DNA mismatch repair (MMR) and removes the thymine but O6-MeG reattaches it again, thus causing replication collapse and formation of double-strand breaks triggering mitochondrial apoptosis [48,91]. Alternatively, TMZ might trigger AP-1 dependent BIM/BAX apoptosis pathway [92], as well as the SIAH1/HIPK2-p53Ser46 pathway [93], thus contributing to intensification or cell death by apoptosis. The sum of these reports strongly suggests that the viscosity might trigger different signaling pathways than substrate elasticity, which potentially might affect not only the effectiveness of anti-cancer drugs, but can also impact the drug resistance development. In our study, we detected some variation in the activation of PI3K pathway, which is well-recognized as a point with a clinical value for expansion of resistance of glioma cells to TMZ treatment [94]. According to our data, glioma cells grown on viscoelastic matrices might develop drug resistance to a lesser extent (Fig. 5D), but it should be more thoroughly explored whether a similar tendency occurs for other drug resistance-associated signaling pathways.

The main limitation of our study is the experimental model that allows to control only one aspect of complex biological environment in which cancers propagate *in vitro*. Literature data indicate that cancer development is also promoted by other non-cancerous cells, such as the cross-linking of blood vessels or the presence of reactive glia, which secrete proteins and growth factors in inflammatory or pathological conditions [95]. However, given that our study is the first to indicate the significant importance of viscosity in lowering the effectiveness of anticancer drugs (temozolomide), we believe that it is reasonable to reduce the number of variables in the experimental model to a minimum, as accurately and reliably as possible to assess the impact of this factor. Our results show that the viscous properties of brain tissue may be clinically relevant and may represent a new class of mechanical factor limiting effectivness of anticancer agents. At the same time, it should be stressed that further development of the experimental *in vitro* brain models accounting for both mechanical and chemical properties of the brain tissue is required to fully understand the significance of the observed phenomena.

5. Conclusions

Evaluation of the cellular response to treatment, using cells growing on substrates with controlled physical properties brings us closer to *in vivo* biomechanical environment and provides a setting that improve the characterization of chemotherapeutic drugs action before animal and clinical trials, which could save research costs and time. Collected data indicate that substrate viscosity affects cell proliferation of untreated cells to a lesser extent, but more significantly alters their morphology and response to chemotherapeutic drug treatment. However, due to the nature of the research further analysis of the influence of viscoelastic properties and surface binding protein needs to be studied with different cell lines to generalize our findings.

CRediT authorship contribution statement

Mateusz Cieśluk: Conceptualization, Methodology, Validation, Formal analysis, Investigation, Data curation, Writing – original draft preparation, Writing – review and editing, Visualization, Funding acquisition. **Ewelina Piktel:** Conceptualization, Methodology, Formal analysis, Data curation, Writing – original draft preparation, Writing – review and editing. **Urszula Wnorowska:** Methodology, Visualization, Writing – review and editing. **Karol Skłodowski:** Formal analysis, Investigation, Writing – review and editing. **Jan Kochanowicz:** Methodology, Formal analysis, Writing – review and editing. **Alina Kułakowska:** Methodology, Formal analysis, Writing – review and editing. **Robert Bucki:** Conceptualization, Methodology, Validation, Writing – original draft preparation, Writing – review and editing, Supervision, Project administration. **Katarzyna Pogoda:** Conceptualization, Methodology, Formal analysis, Writing – review and editing, Visualization, Supervision, Project administration.

Ethical statement

According to Polish regulations, the animals did not require approval from the local ethics committee because they were intended for organ donation.

Data sharing and data accessibility

The data that support the findings of this study are openly available in Bridge of Knowledge Data Repository at https://doi.org/10.34808/x509-nx16 [96].

Declaration of competing interest

The authors declare that they have no known competing financial interests or personal relationships that could have appeared to influence the work reported in this paper.

Data availability

No data was used for the research described in the article.

Acknowledgments

Graphical abstract and schematic figures were created with Biorender.com. This research was funded in whole or in part by National Science Centre, Poland (2021/41/N/NZ7/03966) and Medical University of Bialystok (SUB1/DN/22/004/1122). Study sponsored by a Polpharma Scientific Foundation. For the purpose of open access, the author has applied a CC-BY public copyright license to any Author Accepted Manuscript (AAM) version arising from this submission.

References

[1] A.K. Ommaya, F. Faas, P. Yarnell, Whiplash injury and brain damage: an experimental study, JAMA 204 (1968) 285–289.
[2] M. Pamidi, S. Advani, Nonlinear Constitutive Relations for Human Brain Tissue, 1978.
[3] X. Jin, F. Zhu, H. Mao, M. Shen, K.H. Yang, A comprehensive experimental study on material properties of human brain tissue, J. Biomech. 46 (2013) 2795–2801.
[4] M.C. Murphy, J. Huston 3rd, C.R. Jack Jr., K.J. Glaser, A. Manduca, J.P. Felmlee, R. L. Ehman, Decreased brain stiffness in Alzheimer's disease determined by magnetic resonance elastography, J. Magn. Reson. Imaging 34 (2011) 494–498.
[5] K.J. Streitberger, I. Sack, D. Krefting, C. Pfuller, J. Braun, F. Paul, J. Wuerfel, Brain viscoelasticity alteration in chronic-progressive multiple sclerosis, PLoS One 7 (2012), e29888.
[6] K. Holtzmann, H.O. Gautier, A.F. Christ, J. Guck, R.T. Karadottir, K. Franze, Brain tissue stiffness is a sensitive marker for acidosis, J. Neurosci. Methods 271 (2016) 50–54.
[7] Y. Jamin, J.K.R. Boult, J. Li, S. Popov, P. Garteiser, J.L. Ulloa, C. Cummings, G. Box, S.A. Eccles, C. Jones, J.C. Waterton, J.C. Bamber, R. Sinkus, S.P. Robinson, Exploring the biomechanical properties of brain malignancies and their pathologic determinants in vivo with magnetic resonance elastography, Cancer Res. 75 (2015) 1216–1224.
[8] K. Pogoda, L. Chin, P.C. Georges, F.J. Byfield, R. Bucki, R. Kim, M. Weaver, R. G. Wells, C. Marcinkiewicz, P.A. Janmey, Compression stiffening of brain and its effect on mechanosensing by glioma cells, New J. Phys. 16 (2014), 075002.
[9] S. Nicolle, M. Lounis, R. Willinger, J.F. Palierne, Shear linear behavior of brain tissue over a large frequency range, Biorheology 42 (2005) 209–223.
[10] K. Pogoda, P.A. Janmey, Glial tissue mechanics and mechanosensing by glial cells, Front. Cell. Neurosci. 12 (2018) 25.
[11] M. Cieśluk, K. Pogoda, P. Deptuła, P. Werel, A. Kułakowska, J. Kochanowicz, Z. Mariak, T. Łysoń, J. Reszeć, R. Bucki, Nanomechanics and histopathology as diagnostic tools to characterize freshly removed human brain tumors, Int. J. Nanomedicine 15 (2020) 7509.
[12] I. Sack, B. Beierbach, J. Wuerfel, D. Klatt, U. Hamhaber, S. Papazoglou, P. Martus, J. Braun, The impact of aging and gender on brain viscoelasticity, NeuroImage 46 (2009) 652–657.
[13] R.D. Terry, R. DeTeresa, L.A. Hansen, Neocortical cell counts in normal human adult aging, Ann. Neurol. 21 (1987) 530–539.
[14] D. Takada, H. Nagai, K. Moritake, Y. Akiyama, Edema and elasticity of a fronto-temporal decompressive craniectomy, Surg. Neurol. Int. 3 (2012).
[15] K. Schregel, M.O. Nowicki, M. Palotai, N. Nazari, R. Zane, R. Sinkus, S.E. Lawler, S. Patz, Magnetic resonance elastography reveals effects of anti-angiogenic glioblastoma treatment on tumor stiffness and captures progression in an orthotopic mouse model, Cancer Imaging 20 (2020) 1–16.
[16] G. Ciasca, T.E. Sassun, E. Minelli, M. Antonelli, M. Papi, A. Santoro, F. Giangaspero, R. Delfini, M. De Spirito, Nano-mechanical signature of brain tumours, Nanoscale 8 (2016) 19629–19643.
[17] J.L. Eisenberg, A. Safi, X. Wei, H.D. Espinosa, G.S. Budinger, D. Takawira, S. B. Hopkinson, J.C. Jones, Substrate stiffness regulates extracellular matrix deposition by alveolar epithelial cells, Res. Rep. Biol. 2011 (2011) 1.
[18] F. Chamming's, H. Latorre-Ossa, M.A. Le Frere-Belda, V. Fitoussi, T. Quibel, F. Assayag, E. Marangoni, G. Autret, D. Balvay, L. Pidial, J.L. Gennisson, M. Tanter, C.A. Cuenod, O. Clement, L.S. Fournier, Shear wave elastography of tumour growth in a human breast cancer model with pathological correlation, Eur. Radiol. 23 (2013) 2079–2086.
[19] W. Xu, R. Mezencev, B. Kim, L. Wang, J. McDonald, T. Sulchek, Cell stiffness is a biomarker of the metastatic potential of ovarian cancer cells, PLoS One 7 (2012), e46609.
[20] K. Franze, P.A. Janmey, J. Guck, Mechanics in neuronal development and repair, Annu. Rev. Biomed. Eng. 15 (2013) 227–251.
[21] S.A. Kruse, G.H. Rose, K.J. Glaser, A. Manduca, J.P. Felmlee, C.R. Jack Jr., R. L. Ehman, Magnetic resonance elastography of the brain, NeuroImage 39 (2008) 231–237.
[22] S. Budday, R. Nay, R. de Rooij, P. Steinmann, T. Wyrobek, T.C. Ovaert, E. Kuhl, Mechanical properties of gray and white matter brain tissue by indentation, J. Mech. Behav. Biomed. Mater. 46 (2015) 318–330.
[23] S. Budday, G. Sommer, J. Haybaeck, P. Steinmann, G.A. Holzapfel, E. Kuhl, Rheological characterization of human brain tissue, Acta Biomater. 60 (2017) 315–329.
[24] S. Cheng, E.C. Clarke, L.E. Bilston, Rheological properties of the tissues of the central nervous system: a review, Med. Eng. Phys. 30 (2008) 1318–1337.
[25] L.A. Mihai, L. Chin, P.A. Janmey, A. Goriely, A comparison of hyperelastic constitutive models applicable to brain and fat tissues, J. R. Soc. Interface 12 (2015) 20150486.
[26] G. Seano, H.T. Nia, K.E. Emblem, M. Datta, J. Ren, S. Krishnan, J. Kloepper, M. C. Pinho, W.W. Ho, M. Ghosh, V. Askoxylakis, G.B. Ferraro, L. Riedemann, E. R. Gerstner, T.T. Batchelor, P.Y. Wen, N.U. Lin, A.J. Grodzinsky, D. Fukumura, P. Huang, J.W. Baish, T.P. Padera, L.L. Munn, R.K. Jain, Solid stress in brain tumours causes neuronal loss and neurological dysfunction and can be reversed by lithium, Nat. Biomed. Eng. 3 (2019) 230–245.
[27] V. Umesh, A.D. Rape, T.A. Ulrich, S. Kumar, Microenvironmental stiffness enhances glioma cell proliferation by stimulating epidermal growth factor receptor signaling, PLoS One 9 (2014), e101771.
[28] T.J. Grundy, E. De Leon, K.R. Griffin, B.W. Stringer, B.W. Day, B. Fabry, J. Cooper-White, G.M. O'Neill, Differential response of patient-derived primary glioblastoma cells to environmental stiffness, Sci. Rep. 6 (2016) 1–10.
[29] C. Niu, C.J. Fisher, K. Scheffler, R. Wan, H. Maleki, H. Liu, Y. Sun, C.A. Simmons, R. Birngruber, L. Lilge, Polyacrylamide gel substrates that simulate the mechanical stiffness of normal and malignant neuronal tissues increase protoporphyin IX synthesis in glioma cells, J. Biomed. Opt. 20 (2015), 098002.
[30] S.E. Holt, E.S. Ward, R.J. Ober, D.L. Alge, Shooting for the moon: using tissue-mimetic hydrogels to gain new insight on cancer biology and screen therapeutics, MRS Commun. 7 (2017) 427–441.
[31] C.E. Kandow, P.C. Georges, P.A. Janmey, K.A. Beningo, Polyacrylamide hydrogels for cell mechanics: steps toward optimization and alternative uses, Methods Cell Biol. 83 (2007) 29–46.
[32] B. Babaei, A. Velasquez-Mao, K.M. Pryse, W.B. McConnaughey, E.L. Elson, G. M. Genin, Energy dissipation in quasi-linear viscoelastic tissues, cells, and extracellular matrix, J. Mech. Behav. Biomed. Mater. 84 (2018) 198–207.
[33] E.E. Charrier, K. Pogoda, R.G. Wells, P.A. Janmey, Control of cell morphology and differentiation by substrates with independently tunable elasticity and viscous dissipation, Nat. Commun. 9 (2018) 449.
[34] E.E. Charrier, K. Pogoda, R. Li, C.Y. Park, J.J. Fredberg, P.A. Janmey, A novel method to make viscoelastic polyacrylamide gels for cell culture and traction force microscopy, APL Bioeng. 4 (2020), 036104.
[35] K. Pogoda, E.E. Charrier, P.A. Janmey, A novel method to make polyacrylamide gels with mechanical properties resembling those of biological tissues, Bio-protocol 11 (2021) e4131.
[36] F.G. Davis, S. Freels, J. Grutsch, S. Barlas, S. Brem, Survival rates in patients with primary malignant brain tumors stratified by patient age and tumor histological type: an analysis based on surveillance, epidemiology, and end results (SEER) data, 1973–1991, J. Neurosurg. 88 (1998) 1–10.
[37] R.E. McLendon, E.C. Halperin, Is the long-term survival of patients with intracranial glioblastoma multiforme overstated? Cancer 98 (2003) 1745–1748.
[38] T.A. Wilson, M.A. Karajannis, D.H. Harter, Glioblastoma multiforme: state of the art and future therapeutics, Surg. Neurol. Int. 5 (2014) 64.
[39] C. Alifieris, D.T. Trafalis, Glioblastoma multiforme: pathogenesis and treatment, Pharmacol. Ther. 152 (2015) 63–82.
[40] R. Stupp, M.E. Hegi, W.P. Mason, M.J. van den Bent, M.J. Taphoorn, R.C. Janzer, S. K. Ludwin, A. Allgeier, B. Fisher, K. Belanger, P. Hau, A.A. Brandes, J. Gijtenbeek, C. Marosi, C.J. Vecht, K. Mokhtari, P. Wesseling, S. Villa, E. Eisenhauer, T. Gorlia, M. Weller, D. Lacombe, J.G. Cairncross, R.O. Mirimanoff, Effects of radiotherapy with concomitant and adjuvant temozolomide versus radiotherapy alone on survival in glioblastoma in a randomised phase III study: 5-year analysis of the EORTC-NCIC trial, Lancet Oncol 10 (2009) 459–466.
[41] M.H. Cohen, Y.L. Shen, P. Keegan, R. Pazdur, FDA drug approval summary: bevacizumab (Avastin®) as treatment of recurrent glioblastoma multiforme, Oncologist 14 (2009) 1131–1138.
[42] M. Weller, E. Le Rhun, How did lomustine become standard of care in recurrent glioblastoma? Cancer Treat. Rev. 87 (2020), 102029.
[43] K.J. Wenger, M. Wagner, S.J. You, K. Franz, P.N. Harter, M.C. Burger, M. Voss, M. W. Ronellenfitsch, E. Fokas, J.P. Steinbach, Bevacizumab as a last-line treatment for glioblastoma following failure of radiotherapy, temozolomide and lomustine, Oncol. Lett. 14 (2017) 1141–1146.
[44] U. Herrlinger, T. Tzaridis, F. Mack, J.P. Steinbach, U. Schlegel, M. Sabel, P. Hau, R.-D. Kortmann, D. Krex, O. Grauer, Lomustine-temozolomide combination therapy versus standard temozolomide therapy in patients with newly diagnosed glioblastoma with methylated MGMT promoter (CeTeG/NOA–09): a randomised, open-label, phase 3 trial, Lancet 393 (2019) 678–688.
[45] D.A. Rottenberg, J.Z. Ginos, K.J. Kearfott, L. Junck, D.D. Bigner, In vivo measurement of regional brain tissue pH using positron emission tomography, Ann. Neurol. 15 (Suppl) (1984) S98–S102.
[46] R. Stupp, M.E. Hegi, W.P. Mason, M.J. van den Bent, M.J. Taphoorn, R.C. Janzer, S. K. Ludwin, A. Allgeier, B. Fisher, K. Belanger, P. Hau, A.A. Brandes, J. Gijtenbeek,

C. Marosi, C.J. Vecht, K. Mokhtari, P. Wesseling, S. Villa, E. Eisenhauer, T. Gorlia, M. Weller, D. Lacombe, J.G. Cairncross, R.O. Mirimanoff, E.O.f.R. Groups, T. Treatment of Cancer Brain, O. Radiation, N.C.I.o.C.C.T. Group, Effects of radiotherapy with concomitant and adjuvant temozolomide versus radiotherapy alone on survival in glioblastoma in a randomised phase III study: 5-year analysis of the EORTC-NCIC trial, Lancet Oncol 10 (2009) 459–466.
[47] V. Nikolov, M. Stojanovic, A. Kostic, M. Radisavljevic, N. Simonovic, B. Jelenkovic, L. Berilazic, Factors affecting the survival of patients with glioblastoma multiforme, J. BUON 23 (2018) 173–178.
[48] B. Kaina, M. Christmann, DNA repair in personalized brain cancer therapy with temozolomide and nitrosoureas, DNA Repair (Amst) 78 (2019) 128–141.
[49] L. Kleinberg, S.A. Grossman, S. Piantadosi, M. Zeltzman, M. Wharam, The effects of sequential versus concurrent chemotherapy and radiotherapy on survival and toxicity in patients with newly diagnosed high-grade astrocytoma, Int. J. Radiat. Oncol. Biol. Phys. 44 (1999) 535–543.
[50] A. Schuck, S.B. Müller, A. Köhler, S. Könemann, M. Wienstroer, C. Mosler, C. E. Rübe, H. Wassmann, N. Willich, C. Rübe, Combined radiochemotherapy with paclitaxel in the treatment of malignant glioma, Strahlenther. Onkol. 178 (2002) 486–490.
[51] P. Beauchesne, C. Soler, M. Boniol, T. Schmitt, Response to a phase II study of concomitant-to-sequential use of etoposide and radiation therapy in newly diagnosed malignant gliomas, Am. J. Clin. Oncol. 26 (2003) e22–e27.
[52] D.A. Reardon, J.J. Vredenburgh, A. Coan, A. Desjardins, K.B. Peters, S. Gururangan, S. Sathornsumetee, J.N. Rich, J.E. Herndon, H.S. Friedman, Phase I study of sunitinib and irinotecan for patients with recurrent malignant glioma, J. Neuro-Oncol. 105 (2011) 621–627.
[53] B. Neyns, J. Sadones, C. Chaskis, M. Dujardin, H. Everaert, S. Lv, J. Duerinck, O. Tynninen, N. Nupponen, A. Michotte, J. De Greve, Phase II study of sunitinib malate in patients with recurrent high-grade glioma, J. Neuro-Oncol. 103 (2011) 491–501.
[54] T.T. Batchelor, D.G. Duda, E. di Tomaso, M. Ancukiewicz, S.R. Plotkin, E. Gerstner, A.F. Eichler, J. Drappatz, F.H. Hochberg, T. Benner, D.N. Louis, K.S. Cohen, H. Chea, A. Exarhopoulos, J.S. Loeffler, M.A. Moses, P. Ivy, A.G. Sorensen, P. Y. Wen, R.K. Jain, Phase II study of cediranib, an oral pan-vascular endothelial growth factor receptor tyrosine kinase inhibitor, in patients with recurrent glioblastoma, J. Clin. Oncol. 28 (2010) 2817–2823.
[55] S. Nicolle, M. Lounis, R. Willinger, Shear properties of brain tissue over a frequency range relevant for automotive impact situations: new experimental results, Stapp Car Crash J. 48 (2004) 239.
[56] E. Piktel, I. Ościłowska, Ł. Suprewicz, J. Depciuch, N. Marcińczyk, E. Chabielska, P. Wolak, T. Wollny, M. Janion, M. Parlinska-Wojtan, R. Bucki, ROS-mediated apoptosis and autophagy in ovarian cancer cells treated with Peanut-shaped gold nanoparticles, Int. J. Nanomedicine 16 (2021) 1993–2011.
[57] E. Piktel, I. Prokop, U. Wnorowska, G. Krol, M. Ciesluk, K. Niemirowicz, P. B. Savage, R. Bucki, Ceragenin CSA-13 as free molecules and attached to magnetic nanoparticle surfaces induce caspase-dependent apoptosis in human breast cancer cells via disruption of cell oxidative balance, Oncotarget 9 (2018) 21904–21920.
[58] E. Piktel, I. Oscilowska, Ł. Suprewicz, J. Depciuch, N. Marcińczyk, E. Chabielska, P. Wolak, K. Głuszek, J. Klimek, P.M. Zieliński, Peanut-shaped gold nanoparticles with shells of ceragenin CSA-131 display the ability to inhibit ovarian cancer growth in vitro and in a tumor xenograft model, Cancers 13 (2021) 5424.
[59] E. Piktel, I. Ościłowska, Ł. Suprewicz, J. Depciuch, N. Marcińczyk, E. Chabielska, P. Wolak, T. Wollny, M. Janion, M. Parlinska-Wojtan, ROS-mediated apoptosis and autophagy in ovarian cancer cells treated with peanut-shaped gold nanoparticles, Int. J. Nanomedicine 16 (2021) 1993.
[60] L.T. Li, G. Jiang, Q. Chen, J.N. Zheng, Ki67 is a promising molecular target in the diagnosis of cancer, Mol. Med. Rep. 11 (2015) 1566–1572.
[61] W.-J. Chen, D.-S. He, R.-X. Tang, F.-H. Ren, G. Chen, Ki-67 is a valuable prognostic factor in gliomas: evidence from a systematic review and meta-analysis, Asian Pac. J. Cancer Prev. 16 (2015) 411–420.
[62] T.A. Ulrich, E.M. de Juan Pardo, S. Kumar, The mechanical rigidity of the extracellular matrix regulates the structure, motility, and proliferation of glioma cells, Cancer Res. 69 (2009) 4167–4174.
[63] M. Huml, R. Silye, G. Zauner, S. Hutterer, K. Schilcher, Brain tumor classification using AFM in combination with data mining techniques, Biomed. Res. Int. 2013 (2013), 176519.
[64] K. Schregel, N. Nazari, M.O. Nowicki, M. Palotai, S.E. Lawler, R. Sinkus, P. E. Barbone, S. Patz, Characterization of glioblastoma in an orthotopic mouse model with magnetic resonance elastography, NMR Biomed. 31 (2018), e3840.
[65] J.D. Hughes, N. Fattahi, J.Van Gompel, A. Arani, F. Meyer, G. Lanzino, M.J. Link, R. Ehman, J. Huston, Higher-resolution magnetic resonance elastography in meningiomas to determine intratumoral consistency, Neurosurgery 77 (2015) 653–658, discussion 658–659.
[66] M. Kurt, L. Wu, K. Laksari, E. Ozkaya, Z.M. Suar, H. Lv, K. Epperson, K. Epperson, A.M. Sawyer, D. Camarillo, K.B. Pauly, M. Wintermark, Optimization of a multifrequency magnetic resonance elastography protocol for the human brain, J. Neuroimaging 29 (2019) 440–446.
[67] K.-J. Streitberger, L. Lilaj, F. Schrank, J. Braun, K.-T. Hoffmann, M. Reiss-Zimmermann, J.A. Käs, I. Sack, How tissue fluidity influences brain tumor progression, Proc. Natl. Acad. Sci. 117 (2020) 128–134.
[68] J.S. Aunan-Diop, B. Halle, C.B. Pedersen, U. Jensen, S. Munthe, F. Harbo, M. S. Andersen, F.R. Poulsen, Magnetic resonance elastography in intracranial neoplasms: a scoping review, Top. Magn. Reson. Imaging 31 (2022) 9–22.
[69] S. Koizumi, K. Kurozumi, NI-01 Usefulness of preoperative evaluation of glioma elasticity by the magnetic resonance elastography, Neuro-oncology Advances 2 (2020) ii12.
[70] S.F. Svensson, E. Fuster-Garcia, A. Latysheva, J. Fraser-Green, W. Nordhøy, O. I. Darwish, I.T. Hovden, S. Holm, E.O. Vik-Mo, R. Sinkus, Decreased tissue stiffness in glioblastoma by MR elastography is associated with increased cerebral blood flow, Eur. J. Radiol. 147 (2022), 110136.
[71] K. Pogoda, R. Bucki, F.J. Byfield, K. Cruz, T. Lee, C. Marcinkiewicz, P.A. Janmey, Soft substrates containing hyaluronan mimic the effects of increased stiffness on morphology, motility, and proliferation of glioma cells, Biomacromolecules 18 (2017) 3040–3051.
[72] E.A. Klein, L. Yin, D. Kothapalli, P. Castagnino, F.J. Byfield, T. Xu, I. Levental, E. Hawthorne, P.A. Janmey, R.K. Assoian, Cell-cycle control by physiological matrix elasticity and in vivo tissue stiffening, Curr. Biol. 19 (2009) 1511–1518.
[73] Y. Wang, G. Wang, X. Luo, J. Qiu, C. Tang, Substrate stiffness regulates the proliferation, migration, and differentiation of epidermal cells, Burns 38 (2012) 414–420.
[74] K. Saha, A.J. Keung, E.F. Irwin, Y. Li, L. Little, D.V. Schaffer, K.E. Healy, Substrate modulus directs neural stem cell behavior, Biophys. J. 95 (2008) 4426–4438.
[75] X. Sun, P.D. Kaufman, Ki-67: more than a proliferation marker, Chromosoma 127 (2018) 175–186.
[76] N. Curry, G. Ghezali, G.S. Kaminski Schierle, N. Rouach, C.F. Kaminski, Correlative STED and atomic force microscopy on live astrocytes reveals plasticity of cytoskeletal structure and membrane physical properties during polarized migration, Front. Cell. Neurosci. 11 (2017) 104.
[77] S.M. Lee, T.H. Nguyen, K. Na, I.J. Cho, D.H. Woo, J.E. Oh, C.J. Lee, E.S. Yoon, Nanomechanical measurement of astrocyte stiffness correlated with cytoskeletal maturation, J. Biomed. Mater. Res. A 103 (2015) 365–370.
[78] W.J. Miller, I. Leventhal, D. Scarsella, P.G. Haydon, P. Janmey, D.F. Meaney, Mechanically induced reactive gliosis causes ATP-mediated alterations in astrocyte stiffness, J. Neurotrauma 26 (2009) 789–797.
[79] A.R. Cameron, J.E. Frith, J.J. Cooper-White, The influence of substrate creep on mesenchymal stem cell behaviour and phenotype, Biomaterials 32 (2011) 5979–5993.
[80] K. Gosh, Z. Pan, E. Guan, S. Ge, Y. Liu, T. Nakamura, X. Ren, M. Rafailovich, R. Clark, Cell adaptation to a physiologically relevant ECM mimic with different viscoelastic properties, Biomaterials 28 (2007) 671–679.
[81] T. Boontheekul, E.E. Hill, H.-J. Kong, D.J. Mooney, Regulating myoblast phenotype through controlled gel stiffness and degradation, Tissue Eng. 13 (2007) 1431–1442.
[82] R.E. Jack, C. Blais, C. Scheepers, P.G. Schyns, R. Caldara, Cultural confusions show that facial expressions are not universal, Curr. Biol. 19 (2009) 1543–1548.
[83] J. Feng, Y. Tang, Y. Xu, Q. Sun, F. Liao, D. Han, Substrate stiffness influences the outcome of antitumor drug screening in vitro, Clin. Hemorheol. Microcirc. 55 (2013) 121–131.
[84] C.R.I. Lam, H.K. Wong, S. Nai, C.K. Chua, N.S. Tan, L.P. Tan, A 3D biomimetic model of tissue stiffness interface for cancer drug testing, Mol. Pharm. 11 (2014) 2016–2021.
[85] Y. Shen, X. Wang, J. Lu, M. Salfenmoser, N.M. Wirsik, N. Schleussner, A. Imle, A. F. Valls, P. Radhakrishnan, J. Liang, Reduction of liver metastasis stiffness improves response to bevacizumab in metastatic colorectal cancer, Cancer Cell 37 (2020) 800–817, e807.
[86] M.H. Joyce, C. Lu, E.R. James, R. Hegab, S.C. Allen, L.J. Suggs, A. Brock, Phenotypic basis for matrix stiffness-dependent chemoresistance of breast cancer cells to doxorubicin, Front. Oncol. 8 (2018) 337.
[87] A. Nicolas-Boluda, J. Vaquero, L. Vimeux, T. Guilbert, S. Barrin, C. Kantari-Mimoun, M. Ponzo, G. Renault, P. Deptula, K. Pogoda, Tumor stiffening reversion through collagen crosslinking inhibition improves T cell migration and anti-PD-1 treatment, elife 10 (2021), e58688.
[88] B.W. Miller, J.P. Morton, M. Pinese, G. Saturno, N.B. Jamieson, E. McGhee, P. Timpson, J. Leach, L. McGarry, E. Shanks, Targeting the LOX/hypoxia axis reverses many of the features that make pancreatic cancer deadly: inhibition of LOX abrogates metastasis and enhances drug efficacy, EMBO Mol. Med. 7 (2015) 1063–1076.
[89] J.E. Kim, D.S. Reynolds, M.H. Zaman, M. Mak, Characterization of the mechanical properties of cancer cells in 3D matrices in response to collagen concentration and cytoskeletal inhibitors, Integr. Biol. 10 (2018) 232–241.
[90] B. Kaina, Temozolomide in glioblastoma therapy: role of apoptosis, senescence and autophagy. Comment on strobel et al., temozolomide and other alkylating agents in glioblastoma therapy, Biomedicines 7 (2019).
[91] K. Ochs, B. Kaina, Apoptosis induced by DNA damage O6-methylguanine is Bcl-2 and caspase-9/3 regulated and Fas/caspase-8 independent, Cancer Res. 60 (2000) 5815–5824.
[92] M.T. Tomicic, R. Meise, D. Aasland, N. Berte, R. Kitzinger, O.H. Krämer, B. Kaina, M. Christmann, Apoptosis induced by temozolomide and nimustine in glioblastoma cells is supported by JNK/c-Jun-mediated induction of the BH3-only protein BIM, Oncotarget 6 (2015) 33755–33768.
[93] Y. He, W.P. Roos, Q. Wu, T.G. Hofmann, B. Kaina, The SIAH1-HIPK2-p53ser46 damage response pathway is involved in temozolomide-induced glioblastoma cell death, Mol. Cancer Res. 17 (2019) 1129–1141.
[94] A. Zając, J. Sumorek-Wiadro, E. Langner, I. Wertel, A. Maciejczyk, B. Pawlikowska-Pawlęga, J. Pawelec, M. Wasiak, M. Hułas-Stasiak, D. Bądziul, W. Rzeski,

M. Reichert, J. Jakubowicz-Gil, Involvement of PI3K pathway in glioma cell resistance to temozolomide treatment, Int. J. Mol. Sci. 22 (2021).
[95] D.P. Fitzgerald, D. Palmieri, E. Hua, E. Hargrave, J.M. Herring, Y. Qian, E. Vega-Valle, R.J. Weil, A.M. Stark, A.O. Vortmeyer, Reactive glia are recruited by highly proliferative brain metastases of breast cancer and promote tumor cell colonization, Clin. Exp. Metastasis 25 (2008) 799–810.
[96] M. Cieśluk, Polyacrylamide substrate viscosity impact on temozolomide activity in glioblastoma cells by flow cytometry and rheological measurements, Gdańsk University of Technology, 2022, https://doi.org/10.34808/x509-nx16.